

Detonations at Nanometer Resolution Using Molecular Dynamics

D. W. Brenner, D. H. Robertson, M. L. Elert, and C. T. White^(a)

Naval Research Laboratory, Washington, D.C. 20375-5320

(Received 30 December 1992)

We show that discrete detonation chemistry can be studied using molecular dynamics simulations. A model 2D semi-infinite energetic molecular solid described by reactive many-body potentials is shown to support a chemically sustained shock wave with properties that are consistent with experimental results and the classic continuum theory of planar detonations. These promising results demonstrate for the first time that simulations using reactive many-body potentials provide a powerful probe of the interplay between the continuum properties of shock waves and the atomic-scale chemistry they induce in condensed-phase detonations.

PACS numbers: 82.40.Py, 47.40.Nm, 62.50.+p

Solid explosives rest quietly in their metastable states but when struck can undergo rapid exothermic chemical reactions, often with catastrophic results. Once begun, a detonation propagates as a shock wave inducing the exothermic chemical reactions that sustain it [1]. This shock front separates the unreacted material by only a few lattice spacings from the shocked material which typically experiences pressures of hundreds of kilobars, while flowing at velocities of several kilometers per second [1,2]. Propagating as a shock wave, a detonation consumes the explosive at velocities several times the speed of sound in the quiescent material resulting in the release of chemical energy at rates that can exceed 10^{11} W for a 10 cm^2 detonation front [2].

Processes at condensed-phase shock fronts can occur on such short time (subpicosecond) and length (subnanometer) scales that they are ideal for classical molecular dynamics (MD) simulations [3–5] which follow individual atomic trajectories. Although starting from an atomic-scale description, MD simulations have also proven able to treat enough atoms for long enough times to describe continuum properties of planar shock waves in nonenergetic materials [3]—including such complex hydrodynamic behavior as shock-wave splitting caused by a polymorphic phase transition [4]. Therefore, MD simulations hold great promise both for studying discrete shock-induced chemistry in energetic materials [5] and for directly relating this atomic-scale chemistry to the continuum properties of planar detonations successfully described by the hydrodynamic theory of compressive reactive flows [1,2]. A better understanding of the relationship between atomic-scale chemistry caused by shock waves and the continuum properties of condensed-phase detonations could aid in the design of safer, more reliable explosives.

MD simulations of chemically sustained shock waves, however, require new many-body potentials capable of simultaneously following the dynamics of thousands of atoms in a rapidly changing environment, while including the possibility of exothermic chemical reactions proceeding along chemically reasonable reaction paths from cold solid-state reactants to hot gas-phase molecular products.

In addition, for a molecular solid (which is typical of many energetic materials), these potentials must incorporate both the strong intramolecular forces that bind atoms into molecules and the weak intermolecular forces that bind molecules into solids. In this Letter, we present a model energetic diatomic molecular solid based on many-body potentials that have these key ingredients. Simulations in two dimensions establish that this model can support a chemically sustained shock wave with properties that are intrinsic to the material and consistent with experimental results and the classic Zel'dovich, von-Neumann, and Doering (ZND) continuum theory of planar detonations [1,2]. Remarkably, we find that when a chemically sustained shock wave is achieved, near steady-flow conditions are reached at 50 nm behind the shock front in as little as 15 ps.

To model an energetic solid, we have adapted the empirical-bond-order (EBO) approach introduced by Tersoff to describe static properties of silicon [6]. Although uncomplicated, the EBO potential form has sufficient flexibility to reproduce solid-state properties while retaining the ability to model few-body reactive surfaces [7]. In this approach the binding energy of a system of N atoms is represented in a form reminiscent of pair potentials,

$$E_b = \sum_i \sum_{j>i}^N \{f_c(r_{ij})[V_R(r_{ij}) - \bar{B}_{ij}V_A(r_{ij})] + V_{vdW}(r_{ij})\}, \quad (1)$$

where the functions entering this expression are defined in Table I, r_{ij} is the scalar distance between atoms i and j , and $f_c(r)$ is a cutoff function. The molecular bonding portion of the potential consists of a repulsive, $V_R(r)$, and attractive, $V_A(r)$, term, both modeled by exponentials, while a Lennard-Jones potential, $V_{vdW}(r)$, is used to describe the weak long-range van der Waals interaction. The bond-order function, $\bar{B}_{ij} \equiv (B_{ij} + B_{ji})/2$, introduces many-body effects into the potential by modifying $V_A(r)$ according to the local bonding environment. Hence, \bar{B}_{ij} represents an effective valence which can be tailored through its dependence on environment to describe either highly coordinated metals [8], tetrahedrally bonded semi-

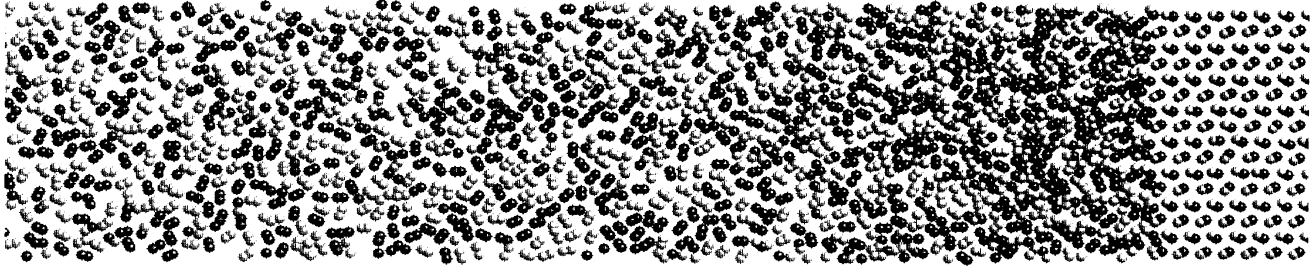


FIG. 1. Snapshot of a chemically sustained shock wave at 15 ps initiated by a four-layer flyer plate with an impact velocity of 6 km/sec. The two types of atoms are depicted in black and white. The shock front is propagating from left to right.

conductors [6], or low-coordination molecular solids with a few strong bonds [4].

Rather than attempt to fit Eq. (1) to a particular system, the parameters given in Table I are chosen to yield a simple generic model of an explosive—a molecular solid composed initially of diatomic AB molecules which, when shocked, might undergo exothermic chemical reactions to form the more stable A_2 and B_2 molecular products. These parameters yield a chemically and physically reasonable model material. First, the exothermic gas-phase half-reactions, $A + AB \rightarrow A_2 + B$ and $B + BA \rightarrow B_2 + A$ —taken as identical in the model—liberate 3.0 eV of energy, similar to the 3.3 eV of energy liberated in the

exothermic reaction $N + NO \rightarrow N_2 + O$ [9] thought to be important in the detonation of nitric oxide. Second, the transition states for these model energetic reactions occur in a collinear geometry as in $H + H_2 \rightarrow H_2 + H$ [10] with an early barrier to reaction which is typical of atom-diatom exothermic reactions. Third, the barrier to reaction is 0.08 eV, similar to the 0.07 eV barrier reported for the exothermic reaction $F + H_2 \rightarrow FH + H$ [11]. Fourth, the vibrational frequencies of the reactant and product molecules at the equilibrium bond distances of 0.12 nm are 1064 cm^{-1} and 1682 cm^{-1} , respectively, and hence are within physical norms. Finally, the inclusion of $V_{\text{vdw}}(r)$ causes the reactants to condense into a molecular solid which in two dimensions has a crystalline binding energy of 0.04 eV per molecule, a distance of closest approach between atoms in nearest-neighbor molecules of 0.33 nm, and a speed of sound of 2 km/s—all physically plausible.

Simulations using this model are initiated by impacting a flyer plate composed of several layers of the unreactive AA molecular solid with the edge of the 2D semi-infinite model diatomic AB molecular crystal initially at rest and at near zero temperature and pressure. The dynamics of the atoms in the system are then propagated by integrating Hamilton's equations of motion with periodic boundary conditions enforced perpendicular to the direction of shock propagation. Doubling the width of the periodic boundary has no significant effect on the results.

Figure 1 depicts a typical snapshot of a chemically sustained shock wave that can result from the flyer-plate impact. A distinct shock front is visible with reactant molecules to the immediate right and many product molecules to the far left. After initiation, this shock front rapidly approaches a constant value of 9.3 km/sec which is within the range of observed detonation velocities [1] and independent of the initiation conditions as demonstrated by the upper three lines in Fig. 2. However, if the flyer-plate velocity is too low, then initiation does not occur and the shock front slows as demonstrated by the two lower lines in Fig. 2. As the number of layers in the flyer plate increases, the impact velocity required for initiation decreases, approaching a limiting value of $\approx 3.9 \text{ km/s}$, consistent with the insensitivity of crystalline explosives to

TABLE I. The components and parameters used in Eq. (1).

$$\begin{aligned}
 V_R(r) &= \frac{D_e}{S-1} \exp[-\alpha\sqrt{2S}(r-r_e)] \\
 V_A(r) &= \frac{SD_e}{S-1} \exp\left[-\alpha\left(\frac{2}{S}\right)^{1/2}(r-r_e)\right] \\
 B_{ij} &= \left\{1 + G \sum_{k \neq i,j} f_c(r_{ik}) \exp[m(r_{ij} - r_{ik})]\right\}^{-n} \\
 f_c(r) &= \begin{cases} 1 & r < 2 \\ \frac{1}{2} \{1 + \cos[\pi(r-2)]\} & 2 \leq r < 3 \\ 0 & 3 \leq r \end{cases} \\
 V_{\text{vdw}}(r) &= \begin{cases} 0 & r < 1.75 \\ P_0 + r[P_1 + r(P_2 + rP_3)] & 1.75 \leq r < 2.91 \\ 4\epsilon \left[\left(\frac{\sigma}{r}\right)^{12} - \left(\frac{\sigma}{r}\right)^6 \right] & 2.91 \leq r < 7.32 \\ 0 & 7.32 \leq r \end{cases}
 \end{aligned}$$

$\text{Mass}_{A,B} = 14.0 \text{ amu}$; $D_e^{AB} = 2.0 \text{ eV}$; $D_e^{AA} = D_e^{BB} = 5.0 \text{ eV}$; $S = 1.8$;
 $\alpha = 27 \text{ nm}^{-1}$; $r_e = 0.12 \text{ nm}$; $G = 5.0$; $n = 0.5$; $m = 22.5 \text{ nm}^{-1}$;
 $\epsilon = 5.0 \times 10^{-3} \text{ eV}$; $\sigma = 0.2988 \text{ nm}$; $P_0 = 4.727 \text{ eV nm}^{-1}$;
 $P_1 = -6.996 \text{ eV nm}^{-1}$; $P_2 = 3.364 \text{ eV nm}^{-1}$;
 $P_3 = -0.520 \text{ eV nm}^{-1}$.

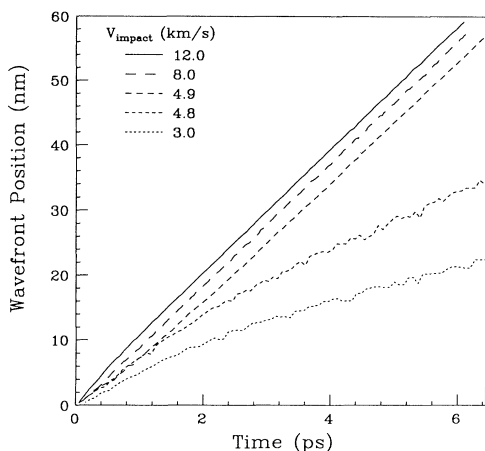


FIG. 2. The positions of the shock front as a function of time for trajectories initiated with four-layer flyer-plate impact velocities of 3.0, 4.8, 4.9, 8.0, and 12.0 km/s.

high velocity impacts [12].

Sectional averages for the pressure, particle velocity, and density as a function of position for the simulation depicted in Fig. 1 are shown in Fig. 3 with the dashed lines denoting their initial values in the undisturbed crystal. These quantities peak at the front and then relax during reaction and expansion behind the shock. The shock-front shape [13] is in accord with expectations based on the classic ZND continuum theory of unsupported planar detonations [1,2] which predicts a von-Neumann point (peak) at the front followed by a reacting flow and a rarefaction (Taylor) wave. The peak pressure [Fig. 3(a)] of 1.0 eV/\AA^2 (corresponding to an effective pressure [14] of approximately 400 kbars) and maximum particle velocity [Fig. 3(b)] of 4.8 km/s are also consistent with a condensed-phase detonation, as is the forward propagating region of product material which develops trailing the shock front [2].

Remarkably, when a chemically sustained shock wave is achieved, the results of the simulations are soon in excellent quantitative agreement with the Rankine-Hugoniot relations [2,15] of continuum theory. These relations state that under steady-flow conditions, in the reference frame where the shock wave is stationary, the quantities, $\bar{\rho} \equiv \rho u$, $\bar{P} \equiv P + \rho u^2$, and $\bar{E} \equiv E + P/\rho + \frac{1}{2} u^2$ are conserved across a planar shock front, provided \bar{E} and \bar{P} are measured far enough behind the shock front that the longitudinal component of the stress tensor equals the hydrostatic pressure and the heat flux vanishes [15]. In these expressions ρ is the density, u is the local particle flow velocity, P is the pressure, and E is the internal energy per unit mass. Figure 4 plots $\bar{\rho}$, \bar{E} , and \bar{P} relative to the shock-front position for simulation times of 5, 10, and 15 ps starting 2 nm behind the shock front. The degree to which these quantities equal their initial values in the unreacted material (dashed lines) at various distances

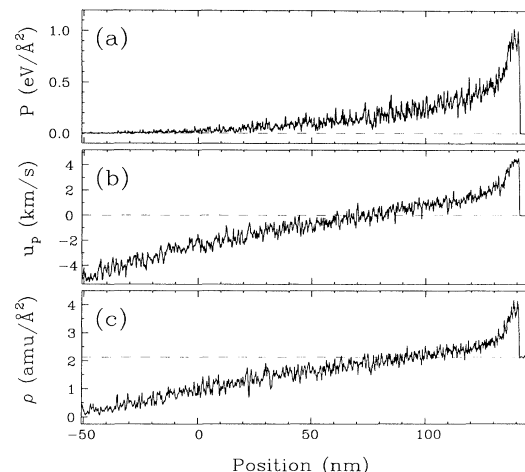


FIG. 3. (a) Sectional averages of the pressure P ; (b) particle flow velocity u_p ; and (c) density ρ , for the simulation depicted in Fig. 1 extended to $0.19 \mu\text{m}$ behind the shock front.

behind the shock front measures how close the simulation is approaching steady flow with an unchanging shock profile across that region. Hence, Fig. 4 shows that these simulations rapidly stabilize close to the shock front (also supported by the rapid relaxation to a constant shock velocity) and then satisfy the Rankine-Hugoniot relations over a progressively wider region reaching near steady-flow conditions 50 nm behind the shock front in as little as 15 ps.

The results in Figs. 1-4 demonstrate that MD simulations can be used both to study discrete shock-induced

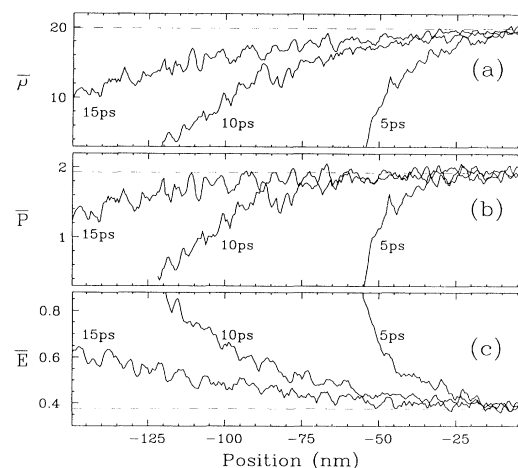


FIG. 4. Plots of the values of $\bar{\rho} \equiv \rho u$, $\bar{P} \equiv P + \rho u^2$, and $\bar{E} \equiv E + P/\rho + \frac{1}{2} u^2$ (in the reference frame where the shock wave is stationary) as a function of distance relative to the shock front at times of 5, 10, and 15 ps for the simulation depicted at 15 ps in Fig. 1. The values in front of the shock wave are shown as dashed lines.

chemistry in energetic materials and to relate this atomic-scale chemistry to the classic ZND continuum theory of planar detonations. Hence, the effects of atomic-scale interactions on the initiation and propagation of chemically sustained shock waves can now be studied in detailed numerical experiments. The EBO potential form can also be extended to model more complex energetic solids [16]. In addition, this potential form can be used to study the role of radical defects thought important in some initiations [17]. Moreover, new numerical algorithms able to follow the dynamics of 10^6 atoms on parallel computers [18] should soon make possible 3D simulations of shocks in these more complex systems [19]. Therefore, MD simulations using reactive many-body potentials represent a promising new tool for probing the relationship between the continuum properties of shock waves and the atomic-scale chemistry they can cause in energetic materials.

This work was supported in part by ONR through NRL and the ONR Physics Division and a grant of computer resources from NRL. D.H.R. acknowledges a NRC-NRL Postdoctoral Research Associateship.

^(a) Author to whom correspondence should be addressed.

- [1] See, e.g., W. C. Davis, *Sci. Am.* **256**, 106 (1987).
- [2] See, e.g., Ya. B. Zel'dovich and A. S. Kompaneets, *Theory of Detonation* (Academic, New York, 1960); W. Fickett and W. C. Davis, *Detonation* (University of California Press, Berkeley, 1979); W. Fickett, *Introduction to Detonation Theory* (University of California Press, Berkeley, 1985), and references therein.
- [3] B. L. Holian, W. G. Hoover, W. Moran, and G. K. Straub, *Phys. Rev. A* **22**, 2798 (1980); A. N. Dremin and V. Yu. Klimenko, *Prog. Astronaut. Aeronaut.* **75**, 253 (1981).
- [4] D. H. Robertson, D. W. Brenner, and C. T. White, *Phys. Rev. Lett.* **67**, 3132 (1991); C. T. White, D. H. Robertson, and D. W. Brenner, *Physica (Amsterdam)* **188A**, 357 (1992).
- [5] A. M. Karo, J. R. Hardy, and F. E. Walker, *Acta Astron.* **5**, 1041 (1978); D. H. Tsai and S. F. Trevino, *J. Chem. Phys.* **81**, 5636 (1984); M. Peyrard, S. Odier, E. Oran, J. Boris, and J. Schnur, *Phys. Rev. B* **33**, 2350 (1986); S. G. Lambrakos, M. Peyrard, E. S. Oran, and J. P. Boris, *Phys. Rev. B* **39**, 993 (1989); M. L. Elert, D. M. Deaven, D. W. Brenner, and C. T. White, *Phys. Rev. B* **39**, 1453 (1989); N. C. Blais and J. R. Stine, *J. Chem. Phys.* **93**, 7914 (1990).
- [6] J. Tersoff, *Phys. Rev. Lett.* **56**, 632 (1986); *Phys. Rev. B* **37**, 6991 (1988).
- [7] D. W. Brenner, *Phys. Rev. B* **42**, 9458 (1990).
- [8] G. C. Abell, *Phys. Rev. B* **31**, 6184 (1985).
- [9] G. M. Barrow, *Physical Chemistry* (McGraw-Hill, New York, 1988), 5th ed., p. 836.
- [10] P. Siegbalm and B. Liu, *J. Chem. Phys.* **68**, 2457 (1978).
- [11] G. C. Fettis, J. H. Knox, and A. F. Trotman-Dickenson, *J. Chem. Soc., London*, 1064 (1960).
- [12] See, e.g., F. P. Bowden and Y. D. Yoffe, *Initiation and Growth of Explosions in Liquids and Solids* (Cambridge Univ. Press, Cambridge, 1985).
- [13] This shape differs qualitatively from the flat-topped, split shock-wave structure we obtained in our preliminary studies [D. W. Brenner, in *Shock Compression of Condensed Matter—1991*, edited by S. C. Schmidt, R. D. Dick, J. W. Forbes, and D. G. Tasker (Elsevier, Amsterdam, 1992), p. 115; D. H. Robertson, D. W. Brenner, M. L. Elert, and C. T. White, in *ibid.*, p. 123]. We have since shown that this flat-topped, split shock-wave structure resulted from a high-pressure, dissociative phase transition unintentionally introduced through our initial parametrizations [C. T. White, D. H. Robertson, M. L. Elert, and D. W. Brenner, in *Microscopic Simulations of Complex Hydrodynamic Phenomena*, edited by M. Mareschal and B. L. Holian (Plenum, New York, 1992), p. 111]. Flat-topped, split shock waves have not been observed in detonating materials.
- [14] This effective 3D pressure is calculated by assuming that the out-of-plane intermolecular distance is the same as the corresponding spacing within the plane.
- [15] Ya. B. Zel'dovich and Yu. P. Raizer, *Physics of Shock Waves and High-Temperature Hydrodynamic Phenomena* (Academic, New York, 1966), Vols. 1 and 2.
- [16] Recently, the EBO potential form has been successfully tailored (Ref. [7]) to describe a range of hydrocarbons (alkanes, alkenes, alkynes, and radicals) and this EBO hydrocarbon potential was used to study C_{60} during hypervelocity impacts with hydrogen-terminated diamond {111} surfaces [R. C. Mowrey, D. W. Brenner, B. I. Dunlap, J. W. Mintmire, and C. T. White, *J. Phys. Chem.* **95**, 7138 (1991)]. Hence, this potential form should have sufficient flexibility to model the rings, strained cages, and radical defects present in complex energetic materials.
- [17] C. B. Storm, R. R. Ryan, J. P. Ritchie, J. H. Hall, and S. M. Bachrach, *J. Phys. Chem.* **93**, 1000 (1989); M. D. Pace and R. Weber, *Mol. Cryst. Liq. Cryst.* **214**, 189 (1992).
- [18] B. L. Holian, A. J. De Groot, W. G. Hoover, and C. G. Hoover, *Phys. Rev. A* **41**, 4552 (1990).
- [19] Especially encouraging in this regard is the relatively short times (< 10 ps) and small sizes ($< 10^4$ atoms) necessary to achieve near steady-flow conditions at the front in our 2D model.